Scanning Microscopy

Volume 1992
Number 6 *Signal and Image Processing in Microscopy and Microanalysis*

Article 18

1992

Simulation for Scanning Electron Microscopy

G. R. Anstis
University of Technology, Sydney, Australia

X. S. Gan
University of Technology, Sydney, Australia

Scanning Microscopy Supplement 6, 1992 (pages 185-193) 0892-953X/92$5.00+.00
Scanning Microscopy International, Chicago (AMF O'Hare), IL 60666 USA

SIMULATION FOR SCANNING ELECTRON MICROSCOPY

G.R. Anstis* and X.S. Gan

Department of Physics, University of Technology, Sydney
Post Office Box 123, Broadway N.S.W. 2007, Australia

Abstract

Simulations of images of surface steps obtained by high energy reflection electron microscopy are presented. It is shown that double images of simple steps, with no associated strain field, may occur when surface resonance conditions are established. Accurate calculation of image intensity requires large calculations and care is needed in relating the computed wave functions to those occurring for a semi-infinite incident wave. Estimates of the time to compute accurate wavefunctions are given and it is shown that they are reasonable for modern fast computers.

Key Words: reflection electron microscopy, simulation, surface resonance, surface steps, high energy electron diffraction.

*Address for Correspondence:
G.R. Anstis,
Department of Physics,
University of Technology, Sydney,
P.O. Box 123,
Broadway,
N.S.W., 2007,
Australia.

Phone No: 61-2-3302193
FAX No: 61-2-3302219

Introduction

Interpretation of electron micrographs usually requires the assistance of simulations because of the strong interaction between the fast electrons and the sample. For the case in which the electrons are incident at grazing angles and it is the reflected electrons which form the image only a limited number of simulations have been performed (e.g. Cowley and Peng, 1985; Ma and Marks, 1990) There is a need to test the reliability of such simulations and to understand any limitations they may have. The images of interest are those of stepped surfaces of crystals and those of crystals with large-period surface structures from which lattice fringes may be obtained (e.g. Koike et al., 1989). Simulation techniques which have been used to analyse diffracted intensities from structures with small unit cells do not appear to be suitable for simulating such images because of their need for large amounts of computer memory. (For a summary of the various methods used in computer simulation see Anstis, 1989; Peng and Whelan, 1990.) Methods of integrating the wave equation which are employed for the simulation of electrons passing through a thin foil may be the most suitable. However when applied to the case of reflection these methods can simulate the interaction of only a narrow beam of incident electrons with a crystal slab of finite thickness. (A recent example of this approach is presented by Lu et al., 1991). How well the methods can simulate the interaction of a broad beam with a very thick crystal should be investigated in a systematic way. This paper presents some results which are relevant to this matter. Since the calculations are quite large they must be performed on a large computer. There is also some benefit in studying simplified models which include only a few Bragg beams.

The system to be considered in this paper is the (110) surface of GaAs oriented so that the (880) Bragg reflection is satisfied and also so that a surface resonance condition is set up. We investigate how efficiently the simulation techniques can be used to determine the electron wavefield that is set up at resonance and we also investigate if the techniques can be used to simulate the double images of steps that are often observed near resonance. Our conclusion is that methods of simulation used for transmission microscopy may be taken over to the case of reflection. We give an estimate of the size of the calculation needed for the accurate simulation of lattice fringe images of surfaces.

Simulation Techniques

High energy electrons are scattered mainly through small angles. This fact may be used to facilitate solving the wave equation describing the fast electrons by reducing Schroedinger's equation to an equation formally similar to a two-dimensional diffusion equation with a complex coefficient of diffusion and the time replaced by a coordinate z, approximately parallel to the direction of incidence.

The electron wave is considered as propagating in a forward direction from one plane to the next plane situated a small distance Δz away. The planes lie approximately perpendicular to the direction of incidence. For the geometry of reflection microscopy these planes are perpendicular to the surface of the crystal.

The terms in the diffusion equation which involve the second partial derivatives with respect to x and y describe the propagation of the wave in the z-direction and they may be evaluated numerically in two different ways. When the wavefunction is periodic on planes perpendicular to the direction of incidence it is most efficient to determine the second derivatives by Fourier transformation of the wavefunction since the operation of differentiation then becomes one of multiplication by the transform parameter. The wavefunction on the plane z is written in the form

$$\Psi(x,y,z) = \exp(2\pi i \mathbf{k}.\mathbf{r}) \sum_{\mathbf{u}} \varphi_{\mathbf{u}}(z) \exp(-2\pi i(u_x x + u_y y)) \quad (1)$$

where $\mathbf{k}$ is the wavevector of the incident wave.

The image intensity on a plane a distance ε beyond the focal plane of the objective lens is

$$I_{\varepsilon}(x,y) = \left| \sum_{\mathbf{u}} A(\mathbf{u}-\mathbf{g}) T_{\varepsilon}(\mathbf{u}-\mathbf{g}) \varphi_{\mathbf{u}}(z) \exp(-2\pi i(u_x x + u_y y)) \right|^2 \quad (2)$$

where $T_{\varepsilon}(\mathbf{u}-\mathbf{g})$ is the transfer function for the objective lens and $A(\mathbf{u}-\mathbf{g})$ is the aperture function which includes only electrons scattered within a certain angular range of the Bragg reflection $\mathbf{g}$.

When the wavefunction is specified on some boundary of the x-y plane, as for example in the case of an electron probe of limited extent, then it is probably best to evaluate the second derivatives in direct space. When the structure has some periodic features, as for a crystal containing a defect, the two approaches can be combined (Howie and Basinski, 1968). and the wavefunction is written in the form

$$\Psi(x,y,z) = \exp(2\pi i \mathbf{k}.\mathbf{r}) \sum_{\mathbf{g}} \psi_{\mathbf{g}}(\mathbf{r}) \exp(-2\pi i \mathbf{g}.\mathbf{r}) \quad (3)$$

Eq.(1) involves a summation over all points $\mathbf{u}$ in reciprocal space perpendicular to z while the summation in eq.(3) is over only reciprocal lattice points $\mathbf{g}$. The coefficients $\varphi_{\mathbf{u}}(z)$ appearing in eq.(1) are functions of z only while the coefficients $\psi_{\mathbf{g}}(\mathbf{r})$ in eq.(3) are functions of x,y and z.

When expansion (3) is used the scattering of the wave is described by a set of coupled partial differential equations, one for each Bragg reflection $\mathbf{g}$. The propagation of the wave in the z direction depends on the excitation errors for the Bragg beams $\mathbf{g}$ and on the the second derivatives with respect to x and y of the functions $\psi_{\mathbf{g}}(\mathbf{r})$. Since these functions do not vary as rapidly with x and y as does the total wavefunction $\Psi(\mathbf{r})$, the computation of the second derivatives does not require too fine a sampling interval.

The intensity of the image formed by placing an objective aperture around Bragg reflection $\mathbf{g}$ and focusing the lens on the plane $z=z_0$ is, to a good approximation for crystals which are not too distorted, given by (Anstis and Cockayne, 1979)

$$I_0(x,y) = |\psi_{\mathbf{g}}(x,y,z_0)|^2 \quad (4)$$

If it is desired to compute the intensity of an out of focus image then the transfer function of the lens must be introduced into the computation.

Images of surface steps have been calculated by making use of the expansion (1) for the wavefunction and calculating the wavefunction on successive planes by using the multi-slice algorithm of Cowley and Moodie (e.g. Peng and Cowley, 1986). The periodicity of the wavefunction $\Psi(x,y,z)$ implied by the discrete summation in eq.(1) means that the wavefunction on the plane z is the result of scattering by a structure periodic in the x-y plane. For the geometry of reflected electrons the periodic structure consists of regions of crystal between regions of empty space. The incident wave then has only finite lateral extent. Except for the case of an incident probe formed in a scanning transmission electron microscope, the width of the wave in the calculations is most likely to be much less than the coherence width of the wave in a transmission microscope.

If calculations of the wavefunction are based on the expansion (3) the same limitation arises since it is necessary to specify the wavefunction on some boundary in the x-y plane. Calculations of this type were first applied to reflected high energy electrons by Anstis (1989).

Matrix methods of calculation do not have this limitation. However the advantages of adopting the methods of computation developed for transmission microscopy are that variations in the surface structure may readily be introduced into the calculation and that the computer memory required is much less.

For a semi-infinite plane wave incident on a perfect surface, the solution to Schroedinger's equation is of the form

$$\Psi(x,y,z) = \exp(2\pi i k_z z) \sum_j a_j(x,y) \exp(-2\pi i \lambda_j x) \quad (5)$$

where the coordinate x is perpendicular to the surface and z is in the surface. Solving the scattering equation for the wavefunction on successive planes may be considered a technique for finding the coefficients $a_j(x,y)$ and the eigenvalues λ_j of a scattering matrix. It is an approach which has been used in other areas of quantum mechanics (Koonin, 1986).

We now present the results of some calculations which illustrate that the methods described above do indeed lead to the same wavefunction obtained by matrix methods of computation, but that the value of z at which a good approximation to the exact solution is obtained depends on the incident and azimuthal angles of the beam. In these calculations the wavefunction on the initial plane z=0 is taken as being uniform outside the crystal and zero inside. The region of vacuum extends 16 nm beyond the crystal surface and the crystal thickness is 4 nm. For the technique involving Fourier expansion (1) in the x and y coordinates, all reciprocal space points within about 20 nm^{-1} of the origin were included in the calculation and the step length in the calculation was 0.2825 nm. The crystal potential was determined using the rigid ion model so that there is not a discontinuous change in the potential at the surface of the crystal. For the technique employing the expansion in

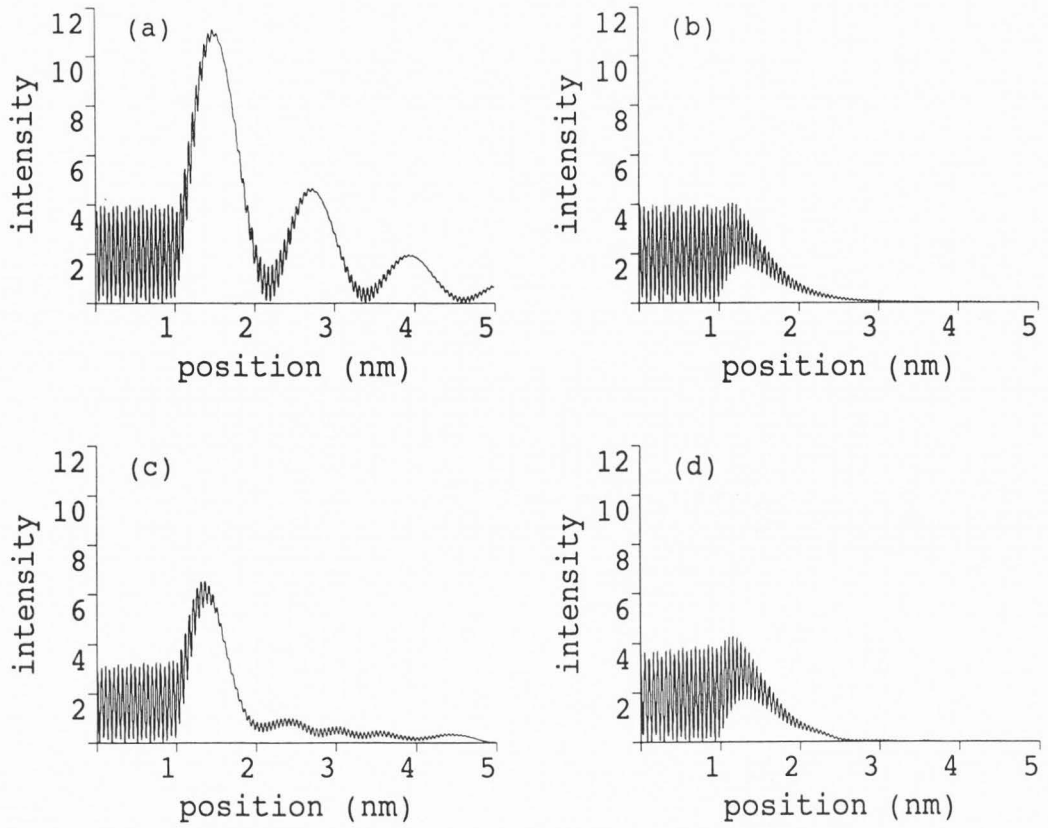

Figure 1. 3-beam calculations of the intensity of the electron wave, averaged over the y direction, as a function of position x perpendicular to the crystal surface. The crystal surface is at 1 nm and the crystal extends to 5 nm. The azimuthal angle is: 27.4 mrad (a,c); 27.8 mrad (b,d). (a) and (b) are solutions, obtained using matrix methods, to the exact form of Schroedinger's equation. (b) and (c) are solutions, on a plane 360 nm from the initial plane, to the equations of Howie and Basinski.

both real and reciprocal space the wave function was sampled every 0.01 nm along lines perpendicular to the surface and the step length was 0.2 nm. Either 3 or 6 Bragg beams and the diffuse scattering associated with them were included in the calculations. The crystal potential was assumed to be that of an infinite crystal right up to the surface and to be zero just outside the crystal (i.e. a deformable ion model of the potential was employed). For calculations based on the Fourier method the effects of inelastic scattering were modelled by introducing an imaginary potential function equal to 1/20th of the real potential. For the other method no absorbing potential was used.

In these calculations the angle of incidence with respect to the surface is 34.8 mrad, at which angle the (880) reflection is satisfied for 100 keV electrons (the lattice parameter is 0.565 nm). The z-direction is [001]. When the azimuthal angle is approximately 27 mrad the (620) beam is satisfied. Under these conditions the (620) beam travels almost parallel to the surface and the intensity of the electron wave just below the surface is very high. A surface resonance condition is established.

Figs. 1(a) and 1(b) show the modulus-squared of the wavefunction, averaged over the y direction (i.e. perpendicular to the plane of the figure) at resonance and just off resonance when only 3 beams (the (000), (880) and (620)) contribute to the wavefunction. The position coordinate in this figure refers to a position on the plane of a detector oriented at right angles to the surface of the crystal. The position 0 nm is furthest from the surface. In Fig. 1 position 1 nm corresponds to the front surface of the crystal and position 5 nm to the back surface. The calculations are based on standard methods of solving the full form of Schroedinger's equation (e.g. Peng and Whelan, 1990). The curves of Figs. 1(c) and 1(d) show the results of integrating the Howie-Basinski scattering equations for 3 beams. The modulus-squared of the wavefunction, averaged over the y direction, is calculated on a plane 360 nm beyond the initial plane. Comparison of Fig. 1(b) with Fig. 1(d) shows that the method can yield the exact solution. However comparing Figs. 1(a) and 1(c) it is seen that this method of solving the scattering equations converges only slowly to the exact wavefunction at the resonance condition. Calculations for a plane 640 nm beyond the initial plane show a wavefunction with a first peak somewhat higher than that shown in Fig. 1(c) and a small second peak at the position of the second peak in the exact wavefunction shown in Fig. 1(a) but other peaks do not appear in the wavefunction on this plane. However the resonance is particularly sharp since only 3 beams are included and no inelastic scattering is allowed for. Thus the model is not expected to correspond to any real system.

Fig. 2 shows the wave function 360 nm beyond the initial plane when the additional beams (220), (400) and (840) are included in the Howie-Basinski equations. The wave field inside the crystal does not extend as far into the

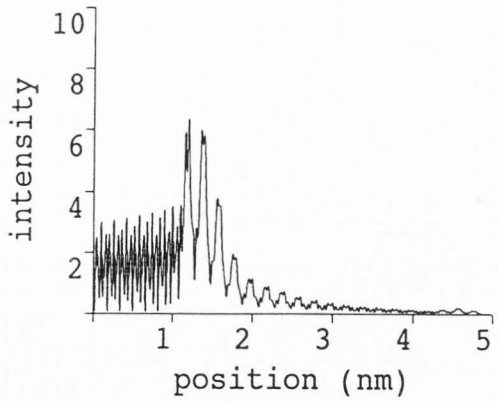

Figure 2. 6-beam calculation, based on the equations of Howie and Basinski, of the total intensity, averaged over the y direction, as a function of position x. The calculations are for a plane 360 nm beyond the initial plane. The crystal surface is at 1 nm and the crystal extends to 5 nm. The azimuthal angle is 28.1 mrad.

crystal as it does for the 3-beam case and it might be expected that convergence to the exact solution would be more rapid. The wavefunction shown in Fig. 2 is similar to that calculated by Lu et al. (1991) using Fourier methods and including all scattering within 20 nm^{-1} of the reciprocal space origin.

Fig. 3 shows the intensities of images formed with the specularly reflected beam (the (880)) at the exact resonance position. The calculations are based on the Howie-Basinski equations and include 3 Bragg beams. The intensity of the image is calculated using eq.(4). For an infinite wave the image intensity is 1. Fig. 3(a) is for a plane 180 nm beyond the initial plane and Fig. 3(b) is for a plane 360 nm beyond the initial plane. The position coordinate in this and all subsequent figures refers to the position on the image plane which lies perpendicular to the direction of the direction of the (880) Bragg reflection. Near the surface (at position 12 nm) the intensity is approximately 0.7 on both planes. The small difference is another indication of the slow rate of convergence of this method of solving Schroedinger's equation near resonance. The intensity should be approximately constant outside the crystal for a distance dependent on the width of the incident wave which has interacted with the crystal. The plot in Fig. 3(a) has this property but not that in Fig. 3(b) where it is seen that the intensity of the reflected wave decreases quickly with distance away from the surface. The reason for this rapid decrease appears to be inaccuracies due to the sampling size used in the calculation. A modification to the algorithm appears to be necessary in order to calculate accurately the wavefunction in the vacuum in reasonable computing times. However the sampling intervals used were in all cases sufficiently small for the accurate calculation of the wavefunction inside the crystal.

Fig. 4 shows the reflected intensity when the azimuthal angle is 0.4 mrad from its value at resonance and should be compared with Fig. 3(b). It is seen that the image intensity near the crystal surface is greater away from resonance than right at resonance. Estimates of the angle at which resonance occurs must take into account not only the variation in calculated intensities with beam orientation but also the dependence on orientation of the value of z beyond which the wavefunction is approximately that expected for a semi-infinite incident wave.

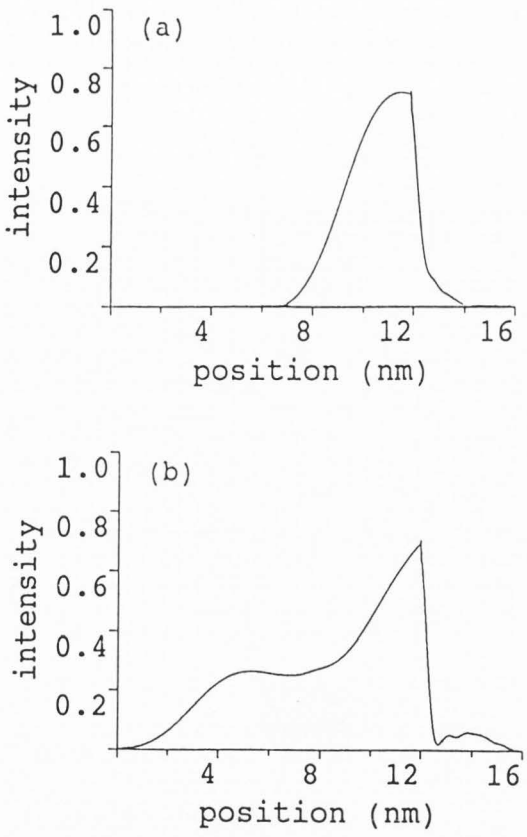

Figure 3. 3-beam calculations, using the Howie-Basinski equations, of the intensity of the image formed with the (880) Bragg reflection as a function of position x. The crystal surface is at 12 nm and the crystal extends to 16 nm. The azimuthal angle is 27.4 mrad. The image plane is: (a) 180 nm; (b) 360 nm beyond the initial plane.

Fig. 5 shows the image intensity calculated using the Fourier approach and including all regions of reciprocal space within 20 nm^{-1} of the origin. The objective aperture is centred on the (880) reflection and its radius is 2.0 nm^{-1}. The lens is focused on a plane 100 nm beyond the initial plane (i.e. the final plane included in the calculation). The direction of the incident beam is a little away from where resonance might be expected. However without performing a matrix type solution to Schroedinger's equation it is difficult to know the exact resonance conditions. The image intensity shows only a slow variation with position away from the surface which is an indication that the Fourier approach does not have the problems of the real space approach in calculating the propagation of the reflected wave.

In summary we see that calculating the propagation of the wave from one plane to another can lead to the exact wavefunction but the rate of convergence may well depend on the direction of incidence. The rate of convergence may well depend on the magnitude of absorption used in the calculation but this point has yet to be investigated in detail.

Simulation of Images of Surface Steps

Experimental images of surface steps obtained under resonance conditions often show double bright or dark lines

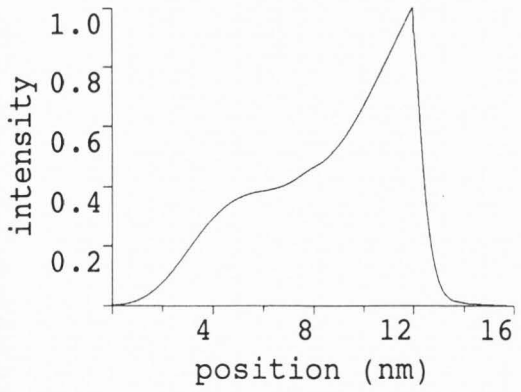

Figure 4. 3-beam calculation, using the Howie-Basinski equations, of the intensity of the image formed with the (880) reflection as a function of position x. The crystal surface is at 12 nm and the crystal extends to 16 nm. The azimuthal angle is 27.8 mrad. The image plane is 360 nm beyond the initial plane.

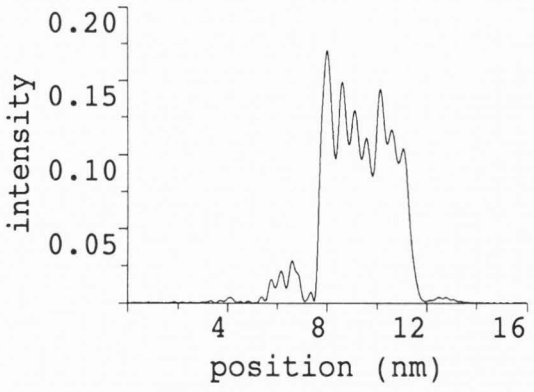

Figure 5. Many-beam calculation, based on the Cowley-Moodie multislice method, of the intensity of the image formed with the (880) beam as a function of position x. The crystal surface is at 12 nm and the crystal extends to 16 nm. The incident angle is 31.7 mrad and the azimuthal angle is 35.7 mrad. The image plane is at 100 nm beyond the initial plane.

(Uchida and Lehmpfuhl, 1987; Peng et al., 1987). An explanation for this phenomenon has been given in terms of the wave propagating just beneath the surface. (Uchida and Lehmpfuhl, 1987; Kambe, 1988; Wang, 1988). An alternative explanation is that at resonance the intensity of the reflected wave is very sensitive to orientation of the crystal and that the double lines arise because of the strain field near a step (Peng and Cowley, 1988).

Here we investigate images, taken at resonance, of an ideal step with no associated strain field. Figs. 6 and 7 show images of up and down steps that have been calculated using the Howie-Basinski equations for a number of azimuthal angles near the resonance condition. The calculated images contain a prominent feature, which does not change shape with changes in azimuthal angle, near position 4 nm, or 8 nm from the surface. The position of this part of the image is just that expected from simple ray optics given that the angle of incidence is 34.8 mrad and that the plane of observation is 240 nm beyond the step. It may be termed the direct image. In the case of an up step (Fig. 6), the direct image consists of two peaks of approximately equal height separated by about 2 nm. The image of the down step (Fig. 7) at a position 8 nm from the surface consists of one strong peak and some subsidiary maxima. The image contrast between the position of the direct image and the surface is strongly peaked at position 8 nm, or 4 nm from the surface, in the case of the up step. The intensity of this peak depends on the diffracting conditions. The calculated images of the down step are somewhat difficult to interpret in terms of intensity maxima and minima. This difficulty is associated with the inaccuracies associated with integrating the Howie-Basinski equations in the vacuum as were discussed above in relation to Figs. 3 and 4. Nevertheless it can be said that the image of the step is not confined to the position predicted from ray optics and that the form of the image is sensitive to the conditions of diffraction. For the same reason a comparison of the relative intensities of the first and second peaks is also difficult.

Calculations of images of steps using Fourier methods (Fig. 8) show some similarities to the three-beam calculations of Figs. 6 and 7, giving support to the interpretation that the image extends a significant distance beyond the geometric position. The radius of the objective aperture used to calculate Fig. 8 is 2 nm^{-1}. The images show fine fringes of spacing 0.5 nm which are not present in the calculations of Figs. 6 and 7 since they are based on the approximation eq.(4) for the image intensity. Comparing Fig. 8(a) with Fig. 6 for the up step we observe a minimum near position 4 nm in all the images and a strong peak closer to the surface. Considering the calculations for a down step, Fig. 8(b) is seen to have a strong peak at about 3.5 nm as do the curves of Fig. 7. There is a minimum at position 8 nm and a weak maximum at 10 nm in Fig. 8(b). Fig. 7(b) has similar features.

The distance from the direct image to any image peak beyond it appears to depend on the diffracting conditions that have been set up. Uchida and Lehmpfuhl (1987) have suggested that the distance between the images can be predicted from the Bloch wave eigenvalues calculated assuming a geometry appropriate for transmission microscopy. A 3-beam Bloch wave calculation for an orientation in which the (880) and (620) beams are approximately satisfied leads to the conclusion that the relevant Bloch waves oscillate with periodicities 36.6 nm and 58.6 nm. The interference of two of these waves produces a periodic variation of 97.2 nm in the total wave and leads to the prediction that the peaks should be separated by 3.4 nm when the angle of incidence of 34.8 mrad is allowed for. The simulated images of Figs. 6 and 7 have peaks separated by approximately this value but the separation appears to vary more rapidly with changes to the azimuthal angle than would be expected from an examination of the eigenvalues.

The conclusion that can be made from these calculations is that near a resonance the image does not depend on just the local structure, an assumption sometimes made when simulating low-resolution images of surfaces (e.g. Peng and Cowley, 1988). It appears then that there are situations in which more detailed calculations of the type presented here may be necessary. The calculations presented above give only semi-quantitative information about images of steps since the incident wave is only 12 nm wide. Calculations based on the Howie-Basinski equations are faster than those based on Fourier expansions of the wavefunction but modifications must be made to the algorithm for the direct space method so that rapid and accurate calculations of the propagation of the reflected wave in free space can be achieved.

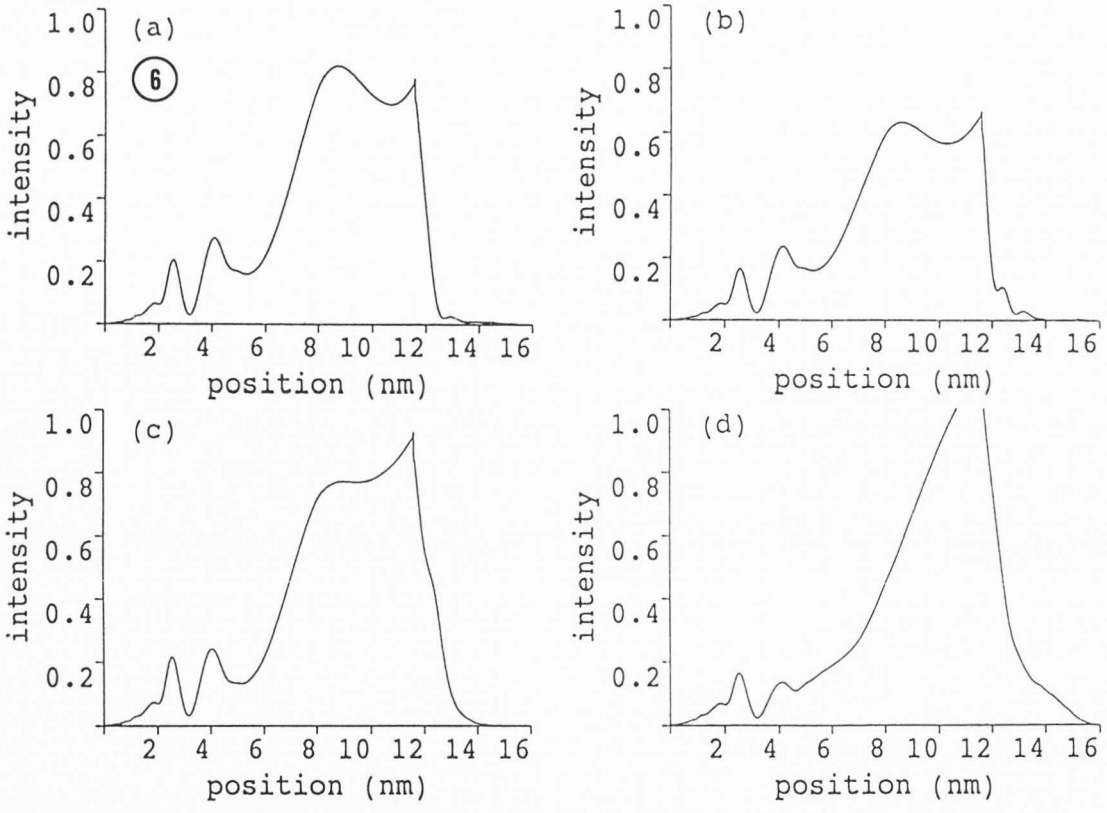
(a)
6
(b)
(c)
(d)
intensity
position (nm)
1.0
0.8
0.6
0.4
0.2
2 4 6 8 10 12 14 16

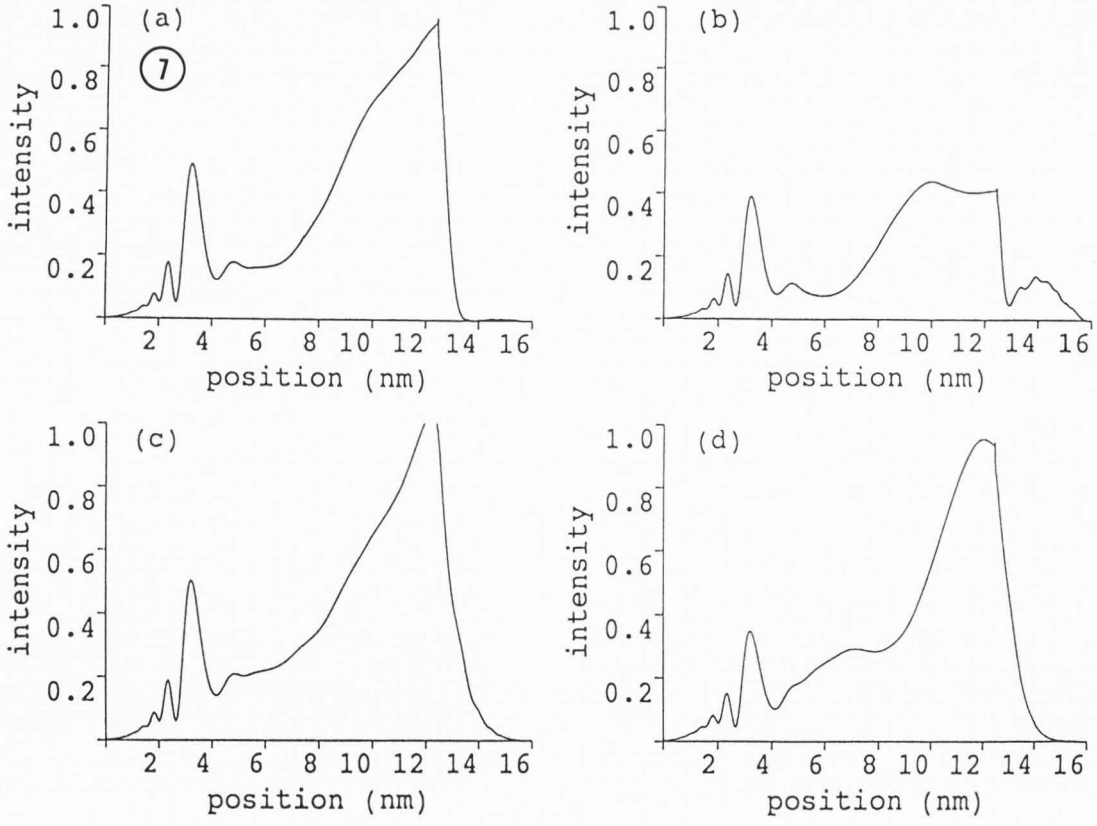
(a)
7
(b)
(c)
(d)
intensity
position (nm)
1.0
0.8
0.6
0.4
0.2
2 4 6 8 10 12 14 16

Figure 6. 3-beam calculations, based on the Howie-Basinski equations, of the image of a 0.4 nm up step. The step is at 120 nm beyond the initial plane and the image plane is 240 nm beyond the step. The crystal surface is at 12 nm and the crystal extends to 16 nm. The azimuthal angles are: (a) 26.7 mrad; (b) 27.4 mrad; (c) 28.1 mrad; (d) 28.9 mrad.

Figure 7. 3-beam calculations, based on the Howie-Basinski equations, of the image of a 0.4 nm down step. Other parameters as for Fig. 6.

Conclusions

The examples shown above suggest that solving Schroedinger's equation by computing the wavefunction on successive planes perpendicular to the surface is efficient enough for carrying out some quantitative comparisons with experimental results. The problem of deciding on how inelastic scattering affects image contrast has not been considered here but the calculations should be no longer for the case of energy-filtered images. The computational method does not require large amounts of computer memory in contrast to methods of solving the full form of Schroedinger's equation. The final part of this paper gives an estimate of the size of the calculation required to simulate a high resolution reflection image of a large unit cell material.

Consider a periodic surface structure with a two dimensional unit cell of dimensions 2.5 nm x 2.5 nm. Assume that calculations with a wave of width 10 nm give a good approximation to the amplitude of the reflected wave when the incident wave is semi-infinite. Further assume that the wave penetrates no further than 10 nm into the crystal. Calculations using the Fourier space technique will involve calculating the wavefunction on planes of dimension 20 nm by 2.5 nm. The step length of the calculation may be 0.25 nm which means that the potential must be sampled 10 times in the direction of integration. The sampling interval of the wavefunction in the planes perpendicular to the surface is determined by the region of the diffraction pattern which contains significant scattering. For instance, in the calculations on GaAs described in the previous sections, scattering out to 20 nm^{-1} is significant. Taking this value as appropriate for the present example means that the sampling should be at 2x20x20 = 800 points in the direction perpendicular to the surface and at 2x20x2.5 = 100 points in a direction parallel to the surface. Arrays of size 1024x128 will be suitable for this example. Each step in the integration of the wave equation requires two Fourier transforms which, using standard fast algorithms, involves approximately $2x4x(1024x128)\log_2(1024x128) = 18 \times 10^6$ multiplications. A supercomputer working at a rate of 500 million floating point operations per second would take about 0.04 s to compute one step in the calculation. In one minute the propagation of the wave through 1500x0.25=375 nm could be computed. The memory requirements for this calculation are those required for storing the wavefunction, the free-space propagator and ten phase gratings. Each involves a complex array of dimension 1024x128 and the total memory is about 3 Mbytes. Additional storage is needed for the fast Fourier transform algorithm. These estimates suggest that it is feasible to use this method for the accurate calculation of waves reflected from structures with large periodicities.

Acknowledgements

The provision of computing time on the Fujitsu Supercomputer of the Australian National University is acknowledged.

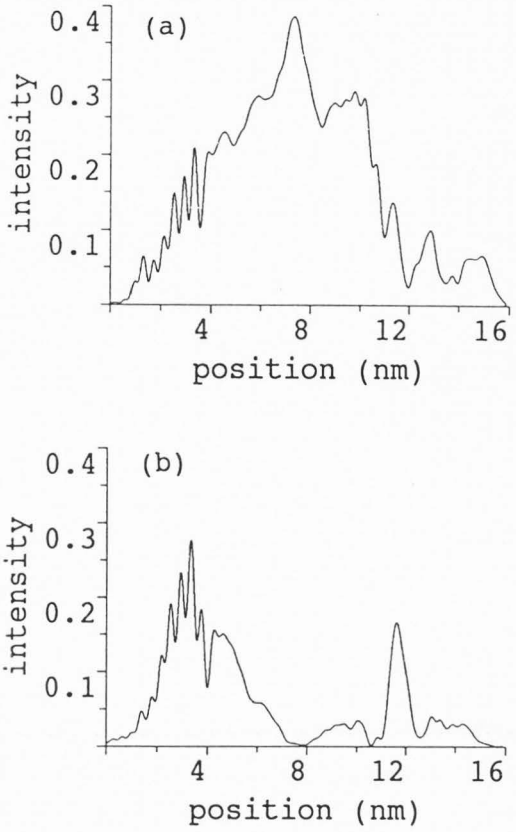

Figure 8. Many-beam calculations, based on the Cowley-Moodie multislice method, for a: (a) 0.4 nm up step and (b) 0.4 nm down step. The step is at 120 nm beyond the initial plane and the image plane is 240 nm beyond the step. The crystal surface is at 12 nm and the crystal extends to 16 nm. The angle of incidence is 34.8 mrad and the azimuthal angle is 28.2 mrad.

References

Anstis GR and Cockayne DJH (1979) "The Calculation and Interpretation of High-Resolution Electron Microscope Images of Lattice Defects", Acta Cryst. A35, 511-524.

Anstis GR (1989) "Simulation Techniques for Reflection Electron Microscopy", in "Computer Simulation of Electron Microscope Diffraction and Images", eds. W. Krakow and M.A. O'Keefe (The Minerals, Metals and Materials Society), 229-238.

Cowley JM and Peng L (1985) "The Image Contrast of Surface Steps in Reflection Electron Microscopy", Ultramicroscopy 16, 59-68.

Howie A and Basinski ZS (1968) "Approximations of the Dynamical Theory of Diffraction Contrast", Philos. Mag. 17, 1039-1063.

Kambe K (1988) "Anomalous Reflected Images of Objects on Crystal Surfaces in Reflection Electron Microscopy", Ultramicroscopy 25, 259-264.

Koike H, Kobayashi K, Ozawa S and Yagi K (1989) "High-Resolution Reflection Electron Microscopy of Si(111)7x7 Surfaces Using a High-Voltage Electron Microscope", Jpn. J. Appl. Phys. 28, 861-865.

Koonin SE (1986) "Computational Physics" (Menlo Park, CA: Benjamin/Cummings Pub. Co.), 176.

Lu P, Liu J and Cowley JM (1991) "Theoretical and Experimental Studies of Electron Resonance Effects in Reflection High- Energy Electron Diffraction", Acta Cryst. A47, 317-327.

Ma Y and Marks LD (1990) "Surface Phenomena in RHEED and REM", Acta Cryst. A46, 594-606.

Peng L-M and Cowley JM (1986) "Dynamical Diffraction Calculations For RHEED and REM", Acta Cryst. A42, 545-552.

Peng L-M, Cowley JM and Hsu T (1987) "Diffraction Contrast in Reflection Electron Microscopy - II. Surface Steps and Dislocations Under the Surface", Micron Microsc. Acta 18, 179-186.

Peng L-M and Cowley JM (1988) "Surface Resonance Efffects and Beam Convergence in REM", Ultramicroscopy 26, 161-168.

Peng L-M and Whelan MJ (1990) "A General Matrix Representation of the Dynamical Theory of Electron Diffraction I. General Theory", Proc. Roy. Soc. A431, 111-123.

Uchida Y and Lehmpfuhl G (1987) "Observation of Double Contours of Monatomic Steps on Single Crystal Surfaces in Reflection Electron Microscopy", Ultramicroscopy 23, 53-60.

Wang ZL (1988) "Dynamical Investigations of Electron Channelling Processes in a Stepped Crystal Surface in Reflection Electron Microscopy", Ultramicroscopy 24, 371-386.

Discussion with Reviewers

J.M. Cowley: As stated, surface steps may show doubled bright or dark lines at resonance conditions. The bright or dark pairs, appearing at the same defocus condition seem to correspond to up-steps or down-steps. The appearance of the doubled lines is seen experimentally to vary with defocus with the doubling most pronounced and both lines of a pair equally sharp near the in-focus condition and asymmetries appearing differently with defocus for the two types of steps. Have you calculated the contrast as a function of defocus?

Authors: Some preliminary calculations have been performed using the parameters of Fig. 8. They show for the focal plane varying from a position 240 nm behind the step to 240 nm in front of the step that the image contrast is greatest when the step is in focus but that for this limited range of conditions of focus there is not a significant change in the shape of the peaks or in their relative heights. Larger calculations should be carried out. With the present set of calculations the interesting features in the image arise a little too close to the leading edge of the reflected wave and to the surface of the crystal to make confident predictions about what might be observed experimentally.

J.M. Cowley: The results of these calculations demonstrate that doubled line images are produced under resonance conditions but a physical picture in terms of energy flow may give a better intuitive idea of what is happening. Can you print out the intensity distributions on successive planes around the step positions for this purpose?

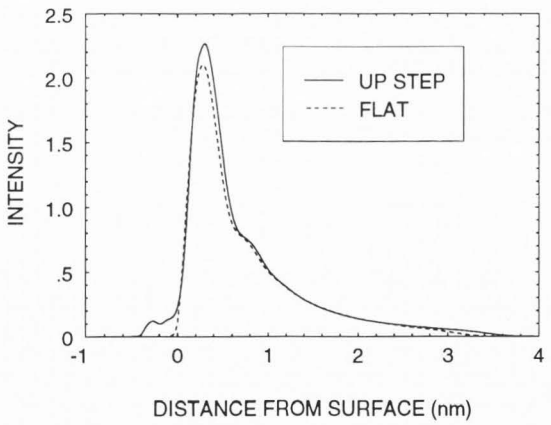

Figure 9. Intensity of that part of the wave travelling approximately parallel to the surface just before a 0.4-nm up step and 10 nm after the step.

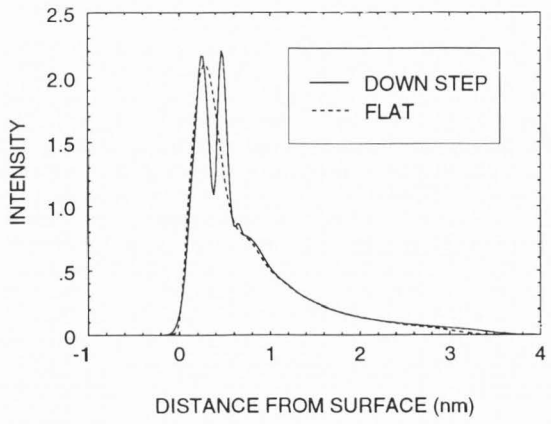

Figure 10. Intensity of that part of the wave travelling approximately parallel to the surface just before a 0.4-nm down step and 10 nm after the step.

Authors: Examples of the intensity distribution just before the wave interacts with a step are shown in Fig. 1. Shown in Figs. 9 and 10 are the intensities of that part of the wave travelling approximately parallel to the surface just before a 0.4 nm-step and on a plane 10 nm beyond the position of the step (Fig. 9 up step; Fig. 10 down step).

Z.L. Wang: In our past experience using the Cowley and Moodie multislice theory for RHEED (reflection high energy electron diffraction) calculations (Wang et al., Ultramicroscopy 23 (1987) 205-222), Fresnel fringes introduced by the sharp window function of the incident beam appear in the vacuum part as the beam gradually approaches the surface, resulting in a non-uniform illumination of the crystal surface. This effect can critically affect the calculated step contrast. How do you eliminate such an artifact in your calculations?

Authors: Our calculated images using the method of Cowley and Moodie (see Figs. 5 and 8) do show oscillations which may arise because of the finite width of the incident beam. In these calculations the leading edge of the incident wave is made to change from 1 to 0 in a smooth way over a distance of 0.5 nm. Looking at Fig. 5,

the calculations for a flat surface, it is seen that the leading edge of the reflected wave is at about position 4 nm (i.e. 8 nm from the surface) but that the reflected wave intensity does not become approximately constant until a portion of the incident wave front approximately 4 nm wide has interacted with the crystal. Even after this amount of interaction the reflected wave has large oscillations in intensity although at a finer scale than the variations in intensity of the step image. When deciding on where the step should be situated for simulation of a stepped surface account was taken of the results shown in Fig. 5. In future calculations it should be situated further beyond the initial plane than it is in the present calculations. In addition an objective aperture smaller than 2 nm^{-1} should be introduced into the simulations to reduce the 0.5-nm oscillations seen in Figs. 5 and 8.

Z.L. Wang: The reasons for observing the double contour effect have been investigated dynamically by Wang (Ultramicroscopy 24 (1988) 371-386). He concluded that the double contour was possibly produced by the interference results of the interrupted surface resonance wave (Wang et al., Ultramicroscopy 27 (1989) 101-112) by the step with the surface reflected wave. How do your calculations compare with his conclusions?
Authors: One of the features of the model proposed in the papers referred to in the question is that at resonance there is a strong surface wave, the amplitude of which varies periodically in the direction of propagation. We indeed find a strongly excited wave in our calculations (Figs. 1 and 2) but we find that the intensity of the wave is constant. The oscillations observed in the simulations presented in these papers may be due to the small width of the incident beam. We believe that the reason for the double contours is related to the amount of interaction between the wave and the crystal which is required to re-establish a wavefield independent of position after the perturbing effects of a step have occurred. Calculations such as those of Figs. 9 and 10 do not indicate that there is any periodic variation of the surface wave after the step.

Z.L. Wang: The REM images are usually taken under the resonance conditions, under which the optimum image contrast could be obtained. The double bright or dark line contrast of a surface step is not often observed . This has recently been shown to be the limited coherence of the electron source (in the literature nearly all the REM images in TEM were taken with a LaB_6 gun). By using a field emission gun (FEG), the image contents and resolution have been significantly improved (Wang and Bentley in: Proc. Annual Meeting of EMSA (1991) 660-661) and the contrast of a surface step shows some residual fringes up to the 4th order. Is it more accurate to compare your calculations with the REM images taken using a FEG?
Authors: Presumably the contrast of images of steps will show oscillations due to the usual Fresnel effects which will be most evident using a FEG. These oscillations might be expected to be fairly independent of the orientation of the surface with respect to the beam. On the other hand the doubled lines observed in a narrow range of conditions near resonance are thought to have a different origin and should not be significantly affected by the coherence of the incident beam. The present calculations do not attempt to take into account the finite coherence width of the beam nor the loss of coherence due to inelastic scattering so it is true to say that they should be compared with images taken using a FEG.